

---

EFDA–JET–PR(04)44

E. Lazzaro, E. Joffrin, R. Coelho, P. Mantica, A.I. Smolyakov, P. Zanca,  
G. Gervasini, M.C.Varischetti and JET EFDA Contributors

# Effect of Electrodynamical Braking Force Localized on Rational Surfaces

# Effect of Electrodynamic Braking Force Localized on Rational Surfaces

E. Lazzaro<sup>1</sup>, E. Joffrin<sup>2</sup>, R. Coelho<sup>4</sup>, P. Mantica<sup>1</sup>, A.I. Smolyakov<sup>5</sup>, P. Zanca<sup>3</sup>,  
G. Gervasini<sup>1</sup>, M.C. Varischetti<sup>1</sup> and JET EFDA Contributors\*

<sup>1</sup>Associazione Euratom-ENEA sulla Fusione, IFP C.N.R., Milan , Italy

<sup>2</sup>Association Euratom-CEA, Cadarache, F-13108, St. Paul lez Durance, France

<sup>3</sup>Associazione Euratom-ENEA sulla Fusione, Consorzio RFX, Padua , Italy

<sup>4</sup>Associação Euratom/IST, Centro de Fusão Nuclear, 1049-001 Lisboa, Portugal

<sup>5</sup>University of Saskatchewan, Saskatoon, Canada

\* See annex of J. Pamela et al, “Overview of Recent JET Results and Future Perspectives”,  
*Fusion Energy 2002 (Proc. IAEA Fusion Energy Conference, Lyon (2002))*.

“This document is intended for publication in the open literature. It is made available on the understanding that it may not be further circulated and extracts or references may not be published prior to publication of the original when applicable, or without the consent of the Publications Officer, EFDA, Culham Science Centre, Abingdon, Oxon, OX14 3DB, UK.”

“Enquiries about Copyright and reproduction should be addressed to the Publications Officer, EFDA, Culham Science Centre, Abingdon, Oxon, OX14 3DB, UK.”



## 1 – Introduction

In recent years, confinement and fusion yield in tokamaks has been significantly increased by forming a core region of reduced anomalous transport called Internal Transport Barrier (ITB) characterized by the rapid appearance of sharp temperature gradients near  $q$  rational surfaces [1].

The appearance of ITBs has been mostly observed to be associated with regions of small or negative magnetic shear ( $s = rq'/q \sim 0$  or  $<0$ ) and recent experiments [1-3], provide evidence that low order rational  $q$ -surfaces play an important role in the formation of ITBs both for reversed and low positive magnetic shear. The different  $q$  profiles are usually obtained in the plasma current ramp-up using various combination of heating schemes. In JET, for example, low positive shear target  $q$  profiles are produced without additional heating or with small level of Ion Cyclotron Resonance Heating (ICRH) power. Strong reversed magnetic shear profiles are formed by pre-heating the plasma with Lower Hybrid Current Drive (LHCD). The combined effect of off-axis current drive and electron heating by the lower hybrid wave can sometimes result in very large value of the safety factor on axis. Although the techniques of tailoring the equilibrium current density profile have made possible the empirical assessment of the conditions for ITB formation, the triggering mechanism and the control of the process, possibly linked with the physical properties of low order rational  $q=m/n$  surfaces, remains somewhat obscure.

Models of turbulent transport lead to conjecture that the onset of ITBs may be related to the modification of the electrostatic potential profile caused by the structure of magnetic island formed by reconnection at rational  $q$  surfaces. This should lead to a variation of the shear of the plasma electric drift velocity in the poloidal direction  $V_{\Box}^{\text{EXB}} = cE^r/B$ . An *accepted* criterion for reduction of the typical scale length of turbulence (and consequent reduction of transport) is that the  $E\Box B$  velocity shear  $V_{\Box}^{\text{EXB}} \geq \Box$ , where  $\Box$  is the typical growth rate of turbulence [1]. We discuss whether a magnetic island, possibly driven by external perturbations, can modify locally  $V_{\Box}^{\text{EXB}}$ , near  $q=m/n$ , in a sufficient and favorable way. It has been suggested that the perturbation forcing reconnection and  $V_{\Box}^{\text{EXB}}$  modification could be provided by mechanisms of mode coupling, possibly involving outer kink-modes with  $m>3$  [2], as this type of MHD activity is often associated with the appearance of an ITB (Fig.1). However this is questionable in terms of overall momentum conservation. On JET (Joint European Torus) experiments of externally driven reconnection have been applying external helical fields by means of

saddle coils on plasma with rotation impressed by 5-8 MW Neutral beam power (NBI) and 5 MW of Ion Cyclotron Wave heating (ICRH) [3].

Experimental evidence shows that reconnection is strongly hindered by plasma rotation and generally *insufficient* to produce the required  $E \times B$  shear perturbation, while naturally occurring ITBs, “anchored” to the  $q=2$  surface are indeed associated with edge MHD signals. In the next two sections we present theoretical arguments that demonstrate the intrinsic limitations of the technique used to trigger ITB’s in a monotonic shear situation.

## 2. Regimes of plasma rotation and magnetic reconnection.

The role of the braking of toroidal rotation velocity by external helical fields resonant at a  $q$ -rational surface can be analyzed in terms of the general response of a reconnecting perturbation in the different regimes of plasma rotation. For clarity and contact with the existing models we recall an established formalism [4] to describe the toroidal momentum balance in terms of the angular toroidal frequency  $\omega = V_\perp / R$  :

$$4\Omega^2 r R_0^3 \frac{\partial \omega}{\partial t} = 4\Omega^2 r R_0^2 S(r, t) + 4\Omega^2 R_0^3 \frac{\partial}{\partial r} \left[ \frac{1}{r} \frac{\partial \omega}{\partial r} \right] + T_{EM}(r, t) \quad (1)$$

with a source profile assigned at time  $t=0$  by the condition  $rS(r) = \Omega R_0 \frac{\partial}{\partial r} \left[ \frac{1}{r} \frac{\partial \omega_0}{\partial r} \right]$  and an electrodynamic torque term  $T_{EM}$  due to externally applied fields with helical pitch resonant with a  $q=m/n$  field line;  $\omega$  is a perpendicular, possibly anomalous momentum diffusion coefficient of the order of  $\Omega^2 a^2 / \tau_E$ , the denominator being the energy confinement time.

The inertial and diffusion operators are linear and the evolution of the differential (“slip”) rotation frequency  $\omega = R^{-1} V_\perp \omega_{coil}$  between the plasma and the perturbation is governed by the equation

$$4\Omega^2 r R_0^3 \frac{\partial \omega}{\partial t} - 4\Omega^2 R_0^3 \frac{\partial}{\partial r} \left[ \frac{1}{r} \frac{\partial \omega}{\partial r} \right] = T_{EM}(r, t) \quad (2)$$

The electrodynamic torque produces a localized braking (acceleration) that locally steepens the gradient of  $\omega$  and consequently of  $V_\perp$ . The question of interest here concerns how steep this gradient can become.

The gradient of  $V_\perp$  in the region where reconnection takes place and profiles tend to flatten, is directly

related to the gradient of  $V_\perp^{\text{EXB}} = \frac{cE^r}{B}$ , since  $\frac{cE^r}{B} = V_\perp \frac{B_\perp}{B} + \frac{c}{en_i Z B} \frac{\partial p}{\partial r} K_i n_i \frac{B_T^2}{B^2} \frac{\partial T_i}{\partial r}$ , and one of

the mechanisms advocated to explain ITBs is the reduction of the typical scale length of turbulence (and consequent reduction of convective transport) occurring when the  $E \times B$  velocity shear  $V_\perp^{\text{EXB}} \geq 0$ ,  $\alpha$  being the typical growth rate of turbulence [2] Other interesting *linear* mechanisms forbidding the onset of turbulence also rely on the existence of a gradient of  $V_\perp$  [5].

The relation of ITBs with the rational surfaces could be due to the electrodynamic torque that is applied locally at the  $q=m/n$  rational surface by some external helical fields and can be modelled as  $T_{\text{EM}}(r, t) = T_\perp(t) \alpha(r \perp r_s)$ .

In section III this aspect will be investigated in some detail, but here we are content of using the *standard* expression for the toroidal torque driven by an external field integrated across a reconnection layer:

$$T_{\perp}^{m,n} = \alpha^2 R_0 \frac{n}{\alpha_0} r_s |V_s| |\alpha_{\text{coil}}| \sin \alpha \quad (3)$$

$$\text{where } \sin \alpha = \frac{\text{Im}[\alpha_{\text{layer}} / (\alpha_{\text{out}})]}{\sqrt{1 + |\alpha_{\text{layer}} / (\alpha_{\text{out}})|^2 + 2 \text{Re}[\alpha_{\text{layer}} / (\alpha_{\text{out}})]}} \quad (4)$$

$\alpha_{\text{out}}$  is the mode natural tearing index and

$$\alpha_{\text{layer}} = \frac{\alpha_{\text{layer}} \alpha_{\text{out}}}{\alpha_s} \quad (5)$$

is the *inner layer* tearing index, generally a function of rotation frequency. Even in the limit of vanishing dissipation it can be shown formally that the presence of a singularity at the  $q(r)=m/n$  surface causes an absorption of torque (and energy).

In general the expression of this localized torque depends on the (differential) plasma rotation  $\alpha = R^\perp V_\perp \alpha_{\text{coil}}$ , and this dependence can be sorted out explicitly on the basis of the asymptotic form of the magnetic flux function in the reconnection layer, that may depend itself on the differential rotation.

A widely accepted form of linear magnetic reconnection response, driven by external fields [4] is obtained from the *layer* asymptotic expressions for the magnetic perturbed flux:

$$\begin{aligned}\Phi_{layer}(r_s^-, t) &= \Phi_s \left( 1 - \frac{1}{2} \frac{\Phi_{coil}}{r_s} |r_s| \right) \quad r < r_s \\ \Phi_{layer}(r_s^+, t) &= \Phi_s \left( 1 + \frac{1}{2} \frac{\Phi_{coil}}{r_s} |r_s| \right) + \Phi_{coil} |r_s| \quad r \geq r_s\end{aligned}\quad (6)$$

where the external “coils” field is represented by  $\Phi_{coil} = \frac{2m}{r_s} \Phi_v$  and  $\Phi_s$  and  $\Phi_{coil}$  are complex valued,

with the appropriate phases  $\phi(t)$  and  $\phi_c(t)$  and  $\Phi_v = I_{ext}$ , the external coils current . Using eqs (1,2) and the other definitions, the *matching* condition, in the lab frame [6], gives

$$\Phi_{layer} = \Phi_{coil} + \frac{|\Phi_{coil}|}{|\Phi_s|} e^{i(\phi_c(t) - \phi(t))} \quad (7)$$

and the *complex* expression of driven reconnected flux is then given by

$$\Phi_s = \frac{2m\Phi_v}{r_s(\Phi_{coil})} \frac{1}{1 + \Phi_{layer}/(\Phi_{coil})} \quad (8)$$

that embodies the dependence of  $\Phi_{layer}$  on frequency.

The complex nature of expressions (7,8) entails the appearance of a phase difference between the driving and driven field perturbations, expressed explicitly by :

$$\tan \Theta = \frac{\text{Im}[\Phi_{layer}/(\Phi_{coil})]}{1 + \text{Re}[\Phi_{layer}/(\Phi_{coil})]} \quad \text{and} \quad \sin \Theta = \frac{\tan \Theta}{\sqrt{1 + \tan^2 \Theta}} \quad (9)$$

The plasma rotation regime has been framed by R. Fitzpatrick into intervals defined by comparison with a certain value  $\Omega_1 \equiv \Omega_A^{2/3} \Omega_B^{2/3} \Omega_0^{1/3}$  [4]. For the present purposes it is sufficient to consider the visco-resistive regime when the slip rotation  $\Omega < \Omega_A^{2/3} \Omega_B^{2/3} \Omega_0^{1/3}$  and the visco-ideal regime prevailing at “high” slip rotation  $\Omega > \Omega_A^{2/3} \Omega_B^{2/3} \Omega_0^{1/3}$ .

It is convenient to recall literally the results of Ref.[4]. In the first case, the linear reconnection theory gives a reconnection layer  $\Phi_{layer} = r_s \Omega_A^{1/3} \Omega_B^{1/6} \Omega_0^{1/6}$  independent of  $\Omega$  , the *complex* tearing layer index is:

$$\Phi_{layer}(\Omega) = i |\Phi_{coil}| \Omega \Phi_{rec} \quad (10)$$

with  $\Phi_{rec} = \frac{2.1036}{|r_s \Phi_{coil}|} \Omega_A^{1/3} \Omega_B^{5/6} \Omega_0^{1/6}$  and the reconnected flux is

$$\Phi_s = \frac{2m\Phi_v / |r_s \Phi_{coil}|}{1 + i \Omega \Phi_{rec}} \quad (11)$$

Then expression (3) becomes

$$T_{\perp}^{m,n} = \frac{1}{2} \Omega^2 R_0 \frac{n}{r_s} \frac{(2m\Omega_v)^2}{|\Omega|} \frac{\Omega \Omega_{rec}}{1 + (\Omega \Omega_{rec})^2} \quad (12)$$

showing a frequency response to a time-periodic magnetic field analogous to that of a metallic conductor with a resistive time constant  $\Omega_{rec}$ . In the visco-ideal regime the relevant expressions are:

$$\Omega_{layer} = |\Omega| \left( \Omega \Omega_{rec} \right)^{1/4} e^{i\Omega t/8}, \quad \Omega = 2.2093(\Omega_1 \Omega_{rec})^{5/4}, \quad \Omega = \text{sign}(\Omega) \quad (13)$$

$$\sin(\Omega) = \frac{\Omega \sin 7\Omega/8}{\sqrt{\Omega^2 + 2\Omega (\Omega \Omega_{rec})^{1/4} \cos 7\Omega/8 + (\Omega \Omega_{rec})^{1/2}}} \quad (14)$$

$$|\Omega_s|^2 = \left| \frac{2m\Omega_v}{r_s} \right|^2 \frac{(\Omega \Omega_{rec})^{1/2}}{\Omega^2 + 2\Omega (\Omega \Omega_{rec})^{1/4} \cos 7\Omega/8 + (\Omega \Omega_{rec})^{1/2}} \quad \text{and} \quad \Omega_{layer} = |\Omega \Omega_{rec}|^{1/4} \frac{2.1036}{|\Omega|} (\Omega_1 \Omega_{rec})^{5/4} \quad (15)$$

and notably the layer width *varies with frequency*.

For  $0 << \Omega_A^{2/3} \Omega_B^{2/3} \Omega_{\perp}^{1/3} \cdot \Omega_{rec} \ll |\Omega \Omega_{rec}| < \Omega$  the expression (3) for the torque, to leading order in  $|\Omega \Omega_{rec}|/\Omega$ , becomes

$$T_{\perp} = \frac{1}{2} \Omega^2 R_0 \frac{n}{r_s} \frac{(2m\Omega_v)^2}{|\Omega|} \frac{(\Omega \Omega_{rec})^{1/4}}{\Omega} \sin 7\Omega/8 \quad (16)$$

where  $\Omega \geq 1$ . The consequences of scaling of the torque with a fractional power of the slip frequency are discussed in the next Section .

### 3. Theory of local toroidal braking.

The toroidal torque, for certain frequency ranges , both in the visco-resistive and in the visco-ideal regimes, has a limiting form with a general scaling

$$T_{\perp} \sim \frac{(\Omega \Omega_{rec})^{\beta}}{\Omega^2 + (\Omega \Omega_{rec})^{\beta}} \quad (\beta=1, 1/4; \Omega=2, 0; \Omega \geq 1) \quad (17)$$

In a range  $|\Omega \Omega_{rec}|^{\beta} < \Omega^2$  these expressions can be effectively linearised with a *negligible* non linear rest.

In these frequency intervals the momentum balance equation admits solutions that to leading order can be factorized  $\Omega \Omega_{rec} = Y(r, t) = A(t)u(r)$  and *therefore* its gradient in the braking region (reconnection

layer) evolves self-similarly: either it exceeds the threshold required for turbulence shearing or it will never do as reconnection proceeds.

In the frequency intervals where the nonlinearities are non negligible (e.g. in the non-monotonic part of the function  $T_0(\Omega)$  [4]) the factorization is not possible at all and therefore the gradient evolves (increasing in absolute value) as reconnection proceeds.

An attractive analytical interpretation is possible. To be definite, in the neighborhood  $|r - r_s| < \Delta_{layer} \ll r_s$ , the e.m. torque is localized and if modelled as a  $\delta$  function the equation of motion may be simplified as

$$4\Omega^2 r_s R_0^3 \frac{\partial \Pi}{\partial t} - 4\Omega^2 R_0^3 \frac{\partial}{\partial r} \left[ r_s \frac{\partial \Pi}{\partial r} \right] K \Pi^{1/4} \delta(r - r_s) = 0 \quad (18)$$

In dimensionless form the equation becomes

$$\frac{\partial y}{\partial \tau} B \frac{\partial^2 y}{\partial x^2} - Cy^{1/4} \delta(x - x_s) = 0 \quad (19)$$

$$\text{with } x = r/a, \quad \tau = t/t_0; \quad y = \Pi / \Omega; \quad B = \frac{\Omega t_0}{a^2}; \quad C = \frac{K}{4\Omega^2 R_0^3 a \tau^{3/4}}$$

Equation (24) is invariant under the one-parameter stretching group transformation

$$\begin{aligned} \Pi &= \tau^{1/3} \Pi \\ r &= \tau r \\ t &= \tau^2 t \end{aligned} \quad (20)$$

therefore it has a similarity solution  $\Pi \propto \frac{t}{\tau}^{2/3} Y \left( \frac{r}{a} \sqrt{\frac{\tau}{t}} \right)$  with  $\Pi \propto a^2 / \tau$  and  $Y(z)$  governed by an

$$\text{equation obtained from eq. (24) introducing the similarity variable } z = \frac{r}{a} \sqrt{\frac{\tau}{t}}.$$

Since  $0 < r < a$ , as time evolves  $z$  spans a narrower range, while  $A(t)$  varies slowly. Therefore locally the profile of  $\Pi \propto A(t)Y(z)$  flattens. In the vicinity of the rational surface, a certain profile of  $\Pi(r,t)$ , with a “hole” due to the external torque, will experience a reduction of the local slope because of viscosity (the local gradient scale length increases  $\mu (t/\tau)^{1/2}$ ) in a trend adverse to the requirements of ITB formation.

Eventually over several viscous times  $\tau$  the rotation will flatten out in any regime. The argument can be tested performing a numerical integration of a (RMHD) quasi-linear model that includes toroidal and poloidal rotation.

From Maxwell and momentum balance equations a RMHD system of equations for the space and time evolution of the magnetic flux perturbations  $\tilde{\Phi}(r,t)\exp(im\tilde{\Phi}nz/R)$  and velocity stream function  $\tilde{u}(r,t)\exp(im\tilde{\Phi}nz/R)$  has been written in large  $R/a$  limit including the evolution of the background toroidal and poloidal velocity fields. The magnetic field is written as  $\mathbf{B} = g\tilde{\Phi}\mathbf{e}_\perp + B_z\mathbf{e}_z$ , with  $g^{\perp 1} = 1 + (nr/mR)^2$  and  $\mathbf{e}_h = \mathbf{e}_z + \mathbf{e}_\perp(nr/mR)$ . and the equations for the background velocity components ( $V_{z0} = \tilde{\Phi}R_0$ ,  $V_{\perp 0} = \tilde{\Phi}a$ ) are:

$$\begin{aligned} \frac{\partial V_{z0}}{\partial t} &= \tilde{\Phi} \cdot \nabla_{\tilde{\Phi}}^{Anom} \left( V_{z0} \frac{\partial V_{z0}}{\partial t} \Big|_{t=0} \right) + \frac{n}{2\tilde{\Phi}_0 R} \text{Im}(\tilde{\Phi}^* \nabla_{\tilde{\Phi}}^2 \tilde{\Phi}) \frac{\tilde{\Phi} n}{2R} \text{Im}(\tilde{u}^* \nabla_{\tilde{\Phi}}^2 \tilde{u}) \\ \frac{\partial V_{\perp 0}}{\partial t} &= \tilde{\Phi} \cdot \nabla_{\tilde{\Phi}}^{Anom} \left( V_{\perp 0} \frac{\partial V_{\perp 0}}{\partial t} \Big|_{t=0} \right) - \frac{m}{2\tilde{\Phi}_0 r} \text{Im}(\tilde{\Phi}^* \nabla_{\tilde{\Phi}}^2 \tilde{\Phi}) + \frac{\tilde{\Phi} m}{2r} \text{Im}(\tilde{u}^* \nabla_{\tilde{\Phi}}^2 \tilde{u}) \nabla_{\tilde{\Phi}}^{neo} \left( V_{\perp 0} \frac{\partial V_{\perp 0}}{\partial t} \Big|_{t=0} \right) \end{aligned}$$

with standard notation for the coefficients. For a given Lundquist number  $S = \tilde{\Phi}_0/\tilde{\Phi}_A$  the calculations show that the relative width  $W/W$  of the region where the e.m. force is applied shrinks as the island grows, so that the effect of perpendicular (anomalous) viscosity on the velocity profile  $V_{\perp}$  prevails.

It is instructive to present the picture of the reconnection and momentum braking process in the quasilinear regime (where the equilibrium evolves) for a model case with plasma equilibrium parameters:  $B_0=1T$ ,  $R_0=3m$ ,  $a=1m$ ,  $n_{e0} = 6 \cdot 10^{19} m^{-3}$  and a relatively flat  $q(r)$  profile with  $q_0=0.7$  and  $q_a=3.1$ . The rational surface  $q=2$  is located at  $r/a=0.79$ .

The Lundquist number is  $S = 2 \cdot 10^7$  and the toroidal angular plasma rotation on frequency axis is  $V_{0z}/2\tilde{\Phi}R_0 = 6\text{kHz}$ ; two regimes of viscosity are considered, with values of the Prandtl number  $\tilde{\Phi} = \tilde{\Phi}_0/\tilde{\Phi}_A \sim 0.05$  and  $\tilde{\Phi} = 5$ . Reconnection at the  $q=m/n$  is driven by the  $(m,n)$  component of the external coils error field.

This field is first ramped up and then kept static at a fixed amplitude (the equivalent coil current is 2.5kA in the low viscosity case and 4 kA in the viscous case).

For the low viscosity case ( $\tilde{\Phi}=0.05$ , visco-resistive regime) in Fig.2 the forced reconnection process is illustrated by the (normalized) island width  $W/a$  growth and the time evolution of the toroidal velocity at the rational surface, being braked by the localized applied torque. From Fig.3 it appears that the mode amplification of Fig.2 is due to the time behaviour of the phase shift between the external field and the mode.

Fig.4 shows that for low Prandtl number the gradient of  $V_{\perp}$  may be large and have a transiently increasing trend in the reconnection region, up to the viscous time-scale. In Fig.5 the radial profile of the total (electromagnetic plus inertial) torque is shown. For high Prandtl number, e.g. for values  $\tilde{\Phi} \sim 5$  (ideal-viscous regime) the reconnection process and evolution of rotation are shown similarly in Figs 6

to 9. The region of braking of the rotation widens and the velocity gradient in vicinity of the rational surface (Fig.8) cannot increase beyond a certain value. It may be concluded that large differential rotation prevents field penetration (and braking torque) in low viscosity regimes, or broadens the braking region at high viscosity. Therefore viscosity opposes the formation of large  $\Delta$  shear near rational surfaces, frustrating the hopes for the ITB onset.

Another physical interpretation can be given in the following terms. The external electromagnetic torque is applied locally. Formally it corresponds to a condition of a finite jump in the velocity derivative across the layer, proportional to the external torque. Thus, it does not define the velocity profile by itself but simply should be considered as a boundary condition. The full profile will be determined by this boundary condition in addition to the other conditions (on the axis and at the plasma edge) by the value of the diffusivity and by the momentum input (if any). The argument can be made that if the plasma is clamped at the rational surface (with external torque) then it is possible to have a strong shear only if the plasma at the other side (boundary or axis) keeps rotating fast. If the rotation is not maintained there the whole plasma will stop [7].

#### 4. Interpretation of some JET experiment.

Spontaneous ITBs in JET occur normally under application of additional power to a reverse shear discharge and is monitored by a sharp increase (above 0.014) of the conventional  $\Delta_T^* = \Delta_s / L_T$  parameter related to the electron temperature gradient length  $L_T$  and ion “sound” larmor radius  $\Delta_s$  [2] (Fig.10, Shot 58315). The typical range of parameters for the spontaneous ITB case was  $I_p=2.2$  MA,  $B_0=2.6$ , line averaged density  $n_e l \sim 10^{19}$  m<sup>-2</sup>, maximum NBI power 12.3 MW, maximum ICRH Power 6.8 MW S  $\sim 2 \cdot 10^8$ . The JET experiments of externally driven reconnection have been done with typical waveforms of the applied saddle coils current shown in Fig.11 (lower) on rotating plasma. The typical range of parameters for this experiment was  $I_p=2.0$  MA,  $B_0=2.6$ ,  $n_e l \sim 10^{19}$  m<sup>-2</sup> maximum NBI power 9.1 MW, and a maximum ICRH power 3.7 MW, with a saddle coils ramp up to  $I_{coil} = 3kA$  3 kA creating a an m=2,n=1 helical magnetic perturbation of intensity  $\frac{\tilde{b}_{crit}^{2,1}}{I_{coil}} 2 \cdot 10^{4} \frac{T}{kA}$ , while the reconnection threshold scales as  $\frac{\tilde{b}_{crit}^{2,1}}{B_0} n^{0.6} B_0^{1.2} \Delta T^{0.5}$  [7]. In both cases S  $\sim 2 \cdot 10^8$ , the confinement time is  $\Delta_E \sim 0.35$  s and the Prandtl number scales as  $\Delta = S(\Delta_A / \Delta_E)$  and is estimated  $\Delta \sim 4$ , close to the model.

The MHD locked mode response shows that above a certain threshold amplitude of the external helical field, a magnetic island is formed (Fig.11 middle) and the expectation was that local braking and simultaneous strong NBI and ICRH power input (Fig.11 upper) would trigger the ITB. The  $\Box^*$  criterion for shot 53820 shows that for driven reconnection (Fig.12) no ITB appears, in contrast with shot 53815 case (Fig.10).

From the previous theoretical considerations and the present observations on JET it should be concluded that in ITB experiments at relatively high temperature and in conditions of high slip rotation (due to NBI) a regime of nearly self-similar braking was entered, unfavorable for onset of ITBs.

The magnetic triggering of ITB's requires therefore a scenario of minimal differential rotation between plasma and external field, as may be obtained with just radio frequency (e.g. ICRH) heating and possibly an oscillating external field that may be made synchronous with the plasma.

## Conclusions

We have isolated one aspect of the complex phenomenon of triggering of ITBs, based on experimental observations, namely that related to externally driven magnetic reconnection, attempted in JET to control the process. Non-trivial aspects of the plasma momentum response to the local electrodynamic torque associated with reconnection driven by external magnetic fields have been found.

## References

- [1] E. Joffrin, et al., Nuc. Fusion **42** (2002) 235-24
- [2] E Joffrin, G Gorini, C D Challis, N C Hawkes, T C Hender, D F Howell, P Maget, P , D Mazon, S E Sharapov, G Tresset, Plasma Phys. Control. Fusion **44** (2002) 1739–1752
- [3] E. Joffrin, C.D. Challis, G.D. Conway, X. Garbet, A. Gude, S. Günter, N.C. Hawkes, T.C. Hender, D.F. Howell, G.T.A. Huysmans, E. Lazzaro, P. Maget, M. Maraschek, A.G. Peeters, S.D. Pinches, S.E. Sharapov, Nucl. Fusion **43** (2003) 1167–1174
- [4] R.Fitzpatrick, Nucl. Fusion **33** 1049 (1993)]
- [5] B. Coppi, E. Lazzaro, M. Lontano, C. Marchetto, “*Ion temperature gradient modes in presence of a sheared flow*” 31<sup>st</sup> EPS Conf. On Plasma Physics and Contr. Fusion, London, 2004
- [6] A.H. Glasser, J.M. Greene, J.L.Johnson, The Phys of Fluids **18**, 875, (1975)
- [7] E. Lazzaro, R. J. Buttery and T. C. Hender, P. Zanca, R. Fitzpatrick, M. Bigi, T. Bolzonella, R. Coelho, M. DeBenedetti, S. Nowak, O. Sauter, Phys. Plasmas, **9**, 3906, (2002)
- [8] A I Smolyakov, E Lazzaro, M Azumi, Y Kishimoto, Plasma Phys. Control. Fusion **43** (2001) 1661–1669

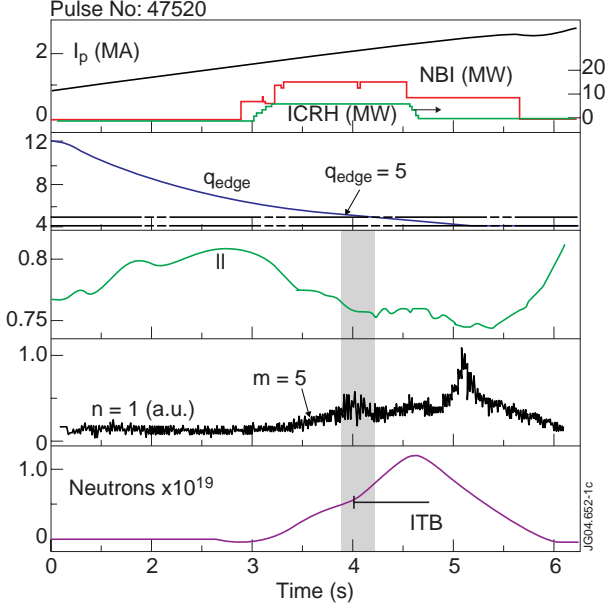


Fig.1.(a)(top): Time trace of plasma current, NBI power, ICRH power in shot 47620; (b)(second): time trace of  $q$  (a) crossing 5 at  $t=4$ ; (c)(third): waveform of internal inductance  $l_i$ ; (d)(fourth): waveform of  $m=5$  MHD signal, showing activity at ITB onset; (e)(bottom): trace on neutron yield, increasing at ITB formation.

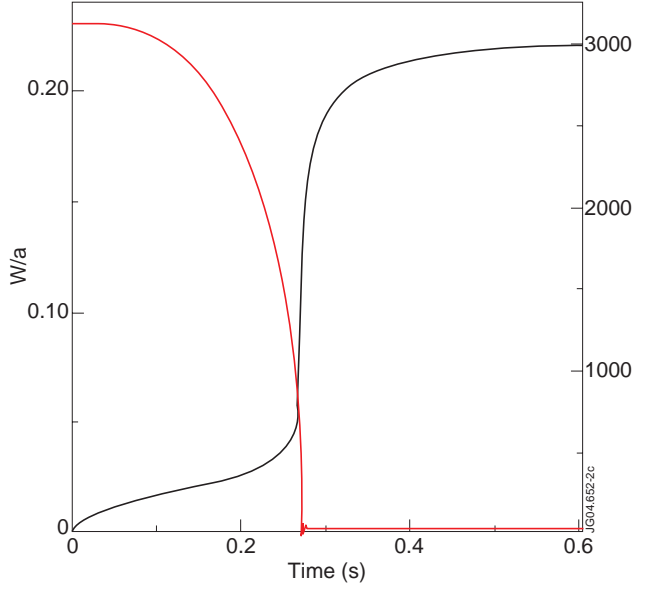


Fig.2: Evolution of the mode amplitude ( $W/a$ , full line) and rotation velocity (dotted line) at the  $q=2$  force ( $S=2 \times 10^7$ ,  $G=0.05$ )

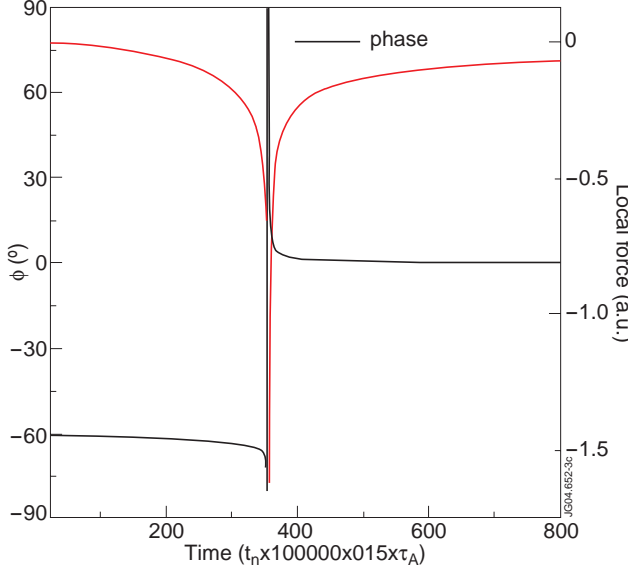


Fig.3: Evolution of the phase shift between external driving field and reconnecting mode(full line), and of the amplitude of the localized electrodynamic force (dotted line), ( $S=2 \times 10^7$ ,  $G=0.05$ )

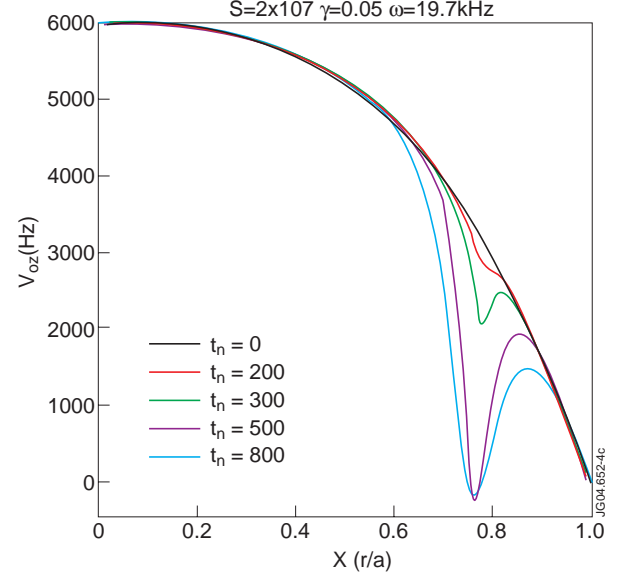


Fig.4: Calculated profile of  $V_z(r,t)$  with localized braking force at low viscosity ( $S=2 \times 10^7$ ,  $G=0.05$ ) at various calculation times  $t_n$ .

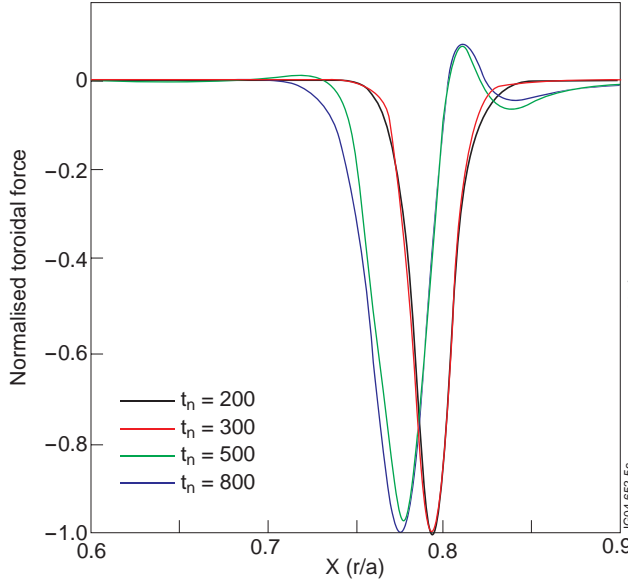


Fig.5: Calculated profile of the (normalized) localized toroidal force at low viscosity ( $S=2*10^7$ ,  $G = 0.05$ ) at various calculation times  $t_n$ .

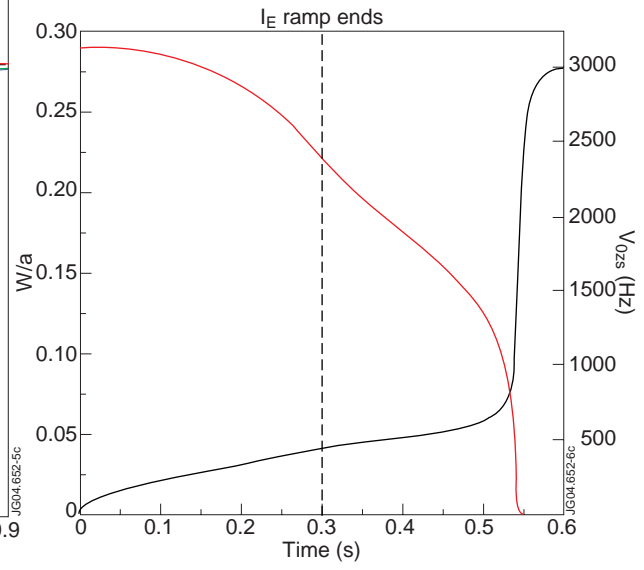


Fig.6: Evolution of the mode amplitude ( $W/a$ , full line) and rotation velocity (dotted line) at the  $q=2$  surface ( $S=2*10^7$ ,  $G = 5$ ).

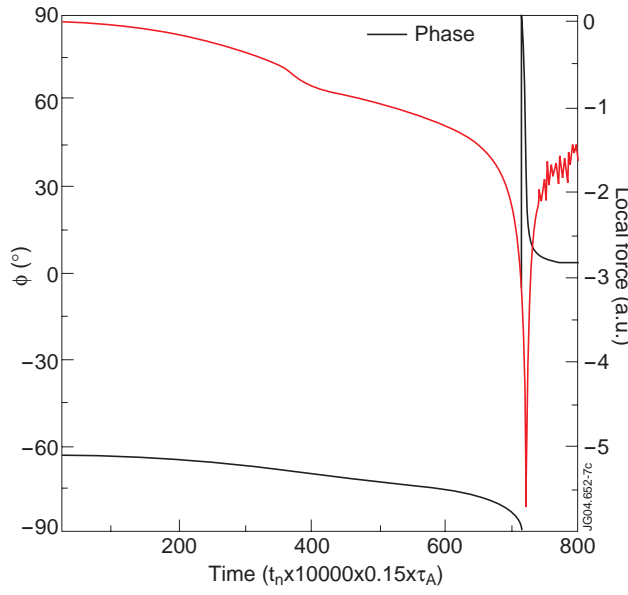


Fig.7: Evolution of the phase shift between external driving field and reconnecting mode (full line), and of the amplitude of the localized electrodynamic force (dotted line) ( $S=2*10^7$ ,  $G = 5$ )

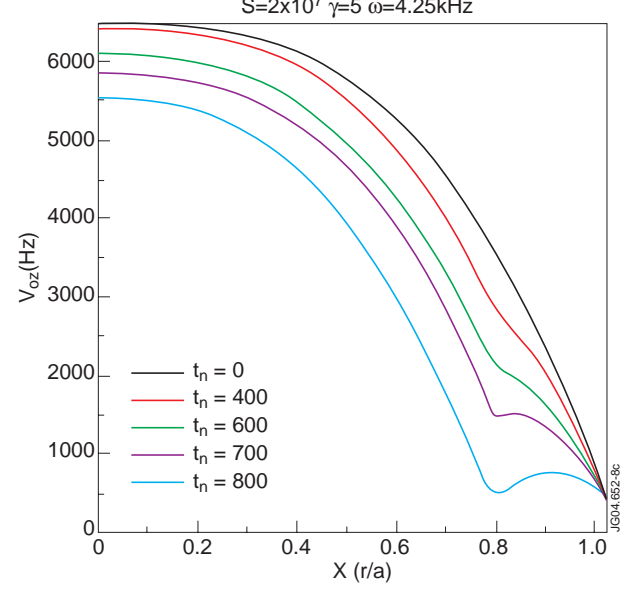


Fig.8: Calculated profile of  $V_z(r,t)$  with localized braking force, at high viscosity; The local shear does not increase ( $S=2*10^7$ ,  $G = 5$ ) at various calculation times  $t_n$

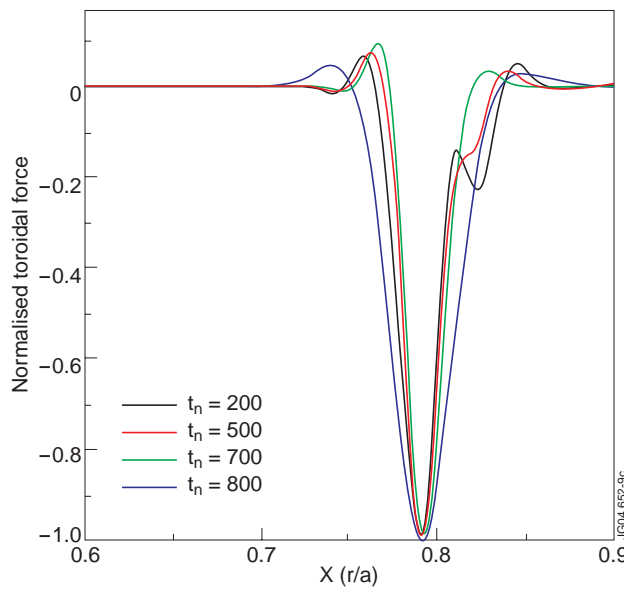


Fig.9: Calculated profile of the (normalized) localized toroidal force at high viscosity ( $S=2*10^7$ ,  $G=5$ ) at various calculation times  $t_n$ .

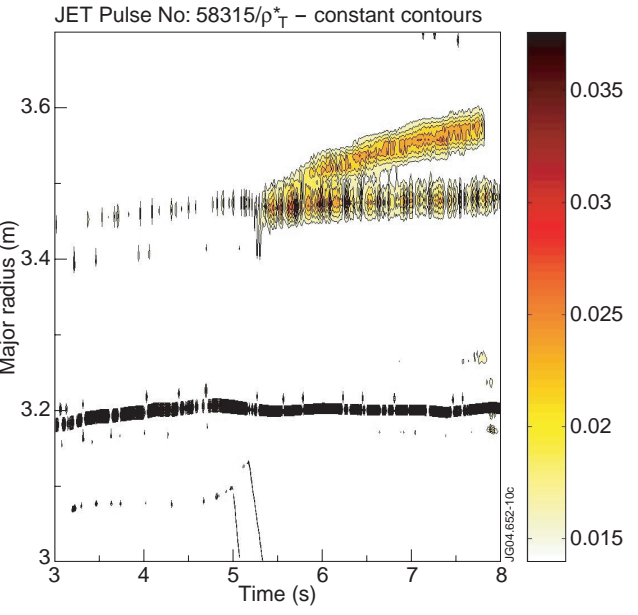


Fig.10: Time trace from experimental data of  $\rho^*$  parameter monitoring a sharp temperature gradient (ITB) appearing spontaneously in JET shot 58320; time is in seconds, starting at 0.

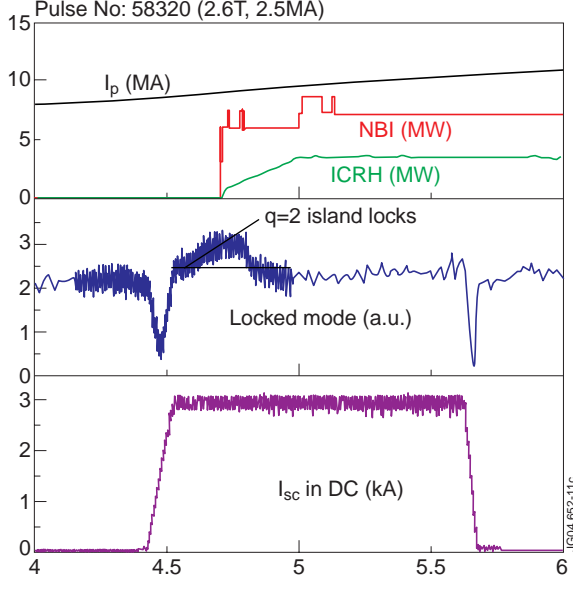


Fig.11.(a)(top): Time trace of plasma current, NBI power, ICRH power in shot 58315; (b)(middle): time trace of MHD pick up coil ( $m=2$   $n=1$  locked mode monitor) tracking the driven reconnection (island formation) when a threshold in external field is exceeded; (c)(bottom): waveform of saddle coils current generating the helical field resonant at  $q=2$ . Time is in seconds, starting at 0.

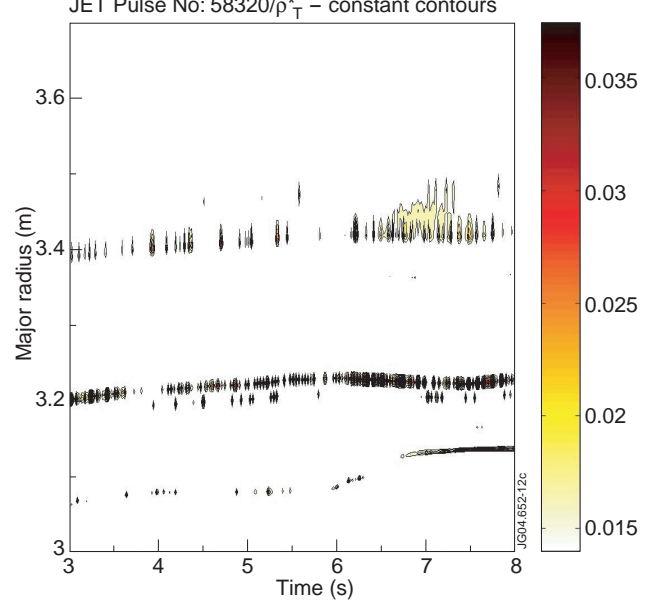


Fig.12: Time trace of the  $\rho^*$  parameter failing to detect an ITB in JET shot 58315 where externally driven island formation was achieved (Fig. 9); time is in seconds, starting at 0.